

SGP: Spotting Groups Polluting the Online Political Discourse

Junhao Wang
junhao.wang@mail.mcgill.ca
CSC McGill, and Mila

Sacha Levy
sacha.levy@mail.mcgill.ca
CSC McGill, and Mila

Ren Wang
renwang435@gmail.com
CSC UBC

Aayushi Kulshrestha
aayushi.kulshrestha@mail.mcgill.ca
CSC McGill, and Mila

Reihaneh Rabbany
rrabba@cs.mcgill.ca
CSC McGill, and Mila

ABSTRACT

Social media sites are becoming a key factor in politics. These platforms are easy to manipulate for the purpose of distorting information space to confuse and distract voters. It is of paramount importance for social media platforms, users engaged with online political discussions, as well as government agencies to understand the dynamics on social media, and identify malicious groups engaging in misinformation campaigns and thus polluting the general discourse around a topic of interest. Past works to identify such disruptive patterns are mostly focused on analyzing user-generated content such as tweets. In this study, we take a holistic approach and propose SGP to provide an informative birds eye view of all the activities in these social media sites around a broad topic and detect coordinated groups suspicious of engaging in misinformation campaigns. To show the effectiveness of SGP, we deploy it to provide a concise overview of polluting activity on Twitter around the upcoming 2019 Canadian Federal Elections, by analyzing over 60 thousand user accounts connected through 3.4 million connections and 1.3 million hashtags. Users in the **polluting groups** detected by SGP-flag are over **4x more likely to become suspended** while majority of these highly suspicious users detected by SGP-flag escaped Twitter's suspending algorithm. Moreover, while few of the **polluting hashtags** detected are **linked to misinformation campaigns**, SGP-signature also flags others that have not been picked up on. More importantly, we also show that a large coordinated set of right-winged conservative groups based in the US are heavily engaged in Canadian politics.

ACM Reference Format:

Junhao Wang, Sacha Levy, Ren Wang, Aayushi Kulshrestha, and Reihaneh Rabbany. 2018. SGP: Spotting Groups Polluting the Online Political Discourse. In *Woodstock '18: ACM Symposium on Neural Gaze Detection, June 03–05, 2018, Woodstock, NY*. ACM, New York, NY, USA, 12 pages. <https://doi.org/10.1145/1122445.1122456>

1 INTRODUCTION

With most of the interaction in our societies moving online, social media websites now play a key role in democracy and politics. It is

Permission to make digital or hard copies of all or part of this work for personal or classroom use is granted without fee provided that copies are not made or distributed for profit or commercial advantage and that copies bear this notice and the full citation on the first page. Copyrights for components of this work owned by others than ACM must be honored. Abstracting with credit is permitted. To copy otherwise, or republish, to post on servers or to redistribute to lists, requires prior specific permission and/or a fee. Request permissions from permissions@acm.org.
Woodstock '18, June 03–05, 2018, Woodstock, NY

© 2018 Association for Computing Machinery.
ACM ISBN 978-1-4503-9999-9/18/06...\$15.00
<https://doi.org/10.1145/1122445.1122456>

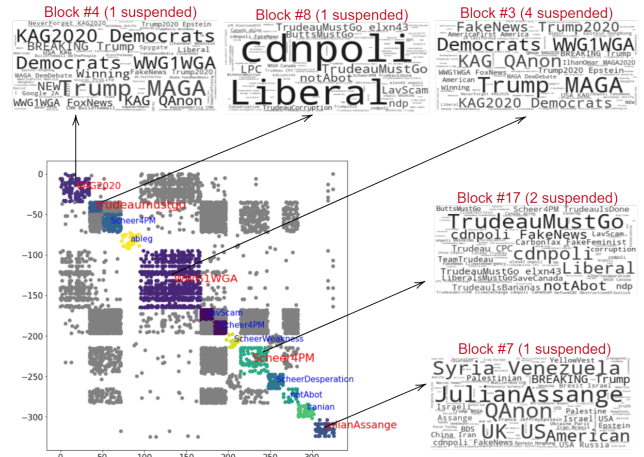


Figure 1: 13 polluting blocks detected by SGP in the Twitter space around the 2019 Canadian Federal Election. The popularity of the hashtags used within these groups reflects the common political creed. The background shows the interactions among these polluting groups through the followership network. We observe a big conservative block of multiple groups with different political creeds, which are heavily engaged with each other which encompasses the Trump MAGA US group and a domestic anti Trudeau group.

becoming clear from recent major political polls that these platforms can be easily manipulated to pollute the information space, from employing bots to generate automated content, to more sophisticated and complex information operation tactics. For example, the 2016 US Presidential Election is believed to have been swayed through interference from Russian trolls and bots [2]. Such operations aim to distort information space to confuse and distract voters, disseminate propaganda and disinformation to foster divisions, and paralyze the decision making abilities of individuals [33]. The ultimate goals or motives of these operations might be hard to interpret, but their effect on public opinion, democracy and elections is clear [16, 3]. Twitter, for example, reported possible engagement of 1.4 billion users with the suspected “trolls” from the Russian government funded Internet Research Agency [23]. Therefore, it is crucial that we develop tools to identify polluting behaviour at an early stage, enabling us to proactively monitor the space and reach a healthy democratic society. Towards this goal, we present a novel approach to study the activity in complex social media space, and identify groups which

are polluting the information space in an unexpectedly organized manner by amplifying each others' voice and boosting each others' influence. More specifically, SGP detects groups of users who are densely being followed by each other and also publish similar content through jointly embedding the connections between the users and the content they post. In extreme cases, bots generated from the same script behave in an almost identical or highly correlated manner [5], and troll or sockpuppets who are being operated by the same person behind the scenes exhibit lock-step behaviour [13]. The main contributions of SGP are four-fold, demonstrated by each of its four components:

- SGP-map **maps out** large scale activity on social media by jointly embedding user connections and the content they post
- SGP-flag **detects** groups of users which are posting similar content and are also densely connected to each other, a common indicator of misinformation campaigns, which we call polluting groups
- SGP-signature **characterizes** the engagement of the polluting groups and finds their political creed
- SGP-meso **explains** how different polluting groups engage with each other and the rest of the population

To demonstrate its effectiveness, we employ the proposed SGP method to spot polluting groups active around the upcoming 2019 federal elections in Canada. In particular, we monitor the activity within Twitter, the most commonly used platforms to mobilize public at the time of political unrest. fig. 1 shows thirteen polluting groups flagged by our proposed SGP in this domain, where fig. 2 shows how these groups engage in the overall discourse around this election.

SGP-map (fig. 1) detects **polluting groups of users which are more than four times more likely to be suspended** by Twitter (explained in detail further in the paper), however, most users skip the current filtering in place whereas evidently behaving strongly similar to the suspended users. On the other end, several of the hashtags these polluting groups use singled out by SGP-signature, **polluting hashtags, are linked to the misinformation campaigns**, in particular #notAbot and #Truedeumustgo [18, 22]. Another key observation made possible by SGP-meso is that there seems to be **a large block of global right wing users** which constitute multiple polluting groups that interact with each other and are highly active in Canadian politics. To the best of our knowledge we are the first group to report this observation, which is made possible through the bird's eye view that SGP-map provides.

While these observations are interesting and help us better navigate the map of twitter activity around this important election, we want to emphasize that **SGP provides a general and novel tool** for computational social science and could be applied to study and investigate polluting groups engaged around any given topic. We verify this through extensive synthetic experiments, to show **scalability** and **effectiveness** of SGP in a controlled setting when the polluting groups are synthetically injected and hence known. Code and more information on data generation and collection are released at <http://removedforblindreview,willbeprovidedwiththecamera-readyversion>

2 PROPOSED METHOD

We model the activity within complex online societies as an attributed graph, in which edges represent connections between the users,

and attributes associated to the nodes encode the content posted by their corresponding user. The main intuition behind this model is that looking at these as a whole, i.e. how users are connected along with the content they post, enables us to infer patterns which only emerge at this higher level. In particular, at this level we would be able to detect and understand the engagement of polluting groups.

More formally, we use a directed attributed graph $G = (\mathcal{V}, \mathcal{E}, \mathbf{X})$, where $|\mathcal{V}| = n$, $\mathbf{X} \in \mathbb{R}^{n \times d}$. Here $\mathcal{V} = \{v_1, v_2, \dots, v_n\}$ represents all the users, \mathcal{E} encodes the followership relationship between them, i.e. $u, v \in \mathcal{E}$ iff user u is followed by user v . The content posted by these users is modeled by \mathbf{X} , where \mathbf{X}_{ij} shows how many times user u_i has posted tweets using hashtag j . We are using the followership and tweets explicitly to better explain this data representation within the context of our application, however, it is straightforward to see that this model is general and can encode any type of connection between users and content they post in other social media platforms. Table 1 summarized this and also presents the list of all symbols we use in this paper.

Given the adjacency matrix \mathbf{A} for graph G , and the attribute matrix \mathbf{X} , we consider a **polluting group** as a group of user which (permuting nodes based on them) **introduces block structure on both \mathbf{A} and \mathbf{X}** . More specifically, we assume G to be generated by a stochastic block model with disjoint partition U_1, \dots, U_K that covers \mathcal{V} , and probability matrix $P \in [0, 1]^{K \times K}$, where P_{ij} is the probability of an edge between nodes in U_i and nodes in U_j . Let an element-wise function $\llbracket f(x) \rrbracket$ transform \mathbf{X} into $\mathbf{X}^b \in \{0, 1\}^{n \times d}$ (e.g. by converting the non-zero elements to 1 which is X_{ik} hashtag k has been used by user i). We also assume \mathbf{X}^b to be modeled by bipartite stochastic block model that has **the same node partition** U_1, \dots, U_K as G , as well as attribute partition W_1, \dots, W_K . We don't require W_1, \dots, W_K to be disjoint or covering all attributes. Based on this construction, we define polluting blocks as subset of node partitions $\{i \in 1 \dots K\}$ such that $j \neq i : P_{ii} \geq \lambda \geq P_{ij}$, where $\lambda \in [0, 1]$ thresholds the edge probability.

Polluting groups do not cover all datapoints, but are in fact a few strikingly dense and small clusters. In particular, **tiny clusters** on the orders of $O(\log n)$ with edge probability much higher than background which is very sparse. Finding these is a challenging task, since even in the decoupled format, the traditional algorithms that recover ground truth partition for bipartite stochastic block model could only discover clusters of size $\Omega(\sqrt{n})$ [19]. With certain assumptions on the dimension and construction of the bipartite graph, the current state of the art provably identifies cluster of size On^ϵ , which is still orders of magnitude greater than $O(\log n)$ [21]. We face a more complex problem since the partitions need to be jointly dense in both the stochastic block model for adjacency matrix, as well as bipartite stochastic model for binarized attribute matrix.

SGP is able to effectively recover these tiny clusters through an embedding-based dense block detection, which first jointly embeds the data onto Euclidean space, and then applies a centroid or density based clustering algorithm to find polluting blocks. We explain the four core component of SGP in the following:

SGP-map first **jointly embeds** \mathcal{V}, \mathcal{E} and \mathbf{X} of G into \mathbf{H} by preserving one-hop neighborhood structural similarity and attribute information. This is done through two steps: (1) project \mathbf{X} on its first k left singular vectors using truncated singular value decomposition;

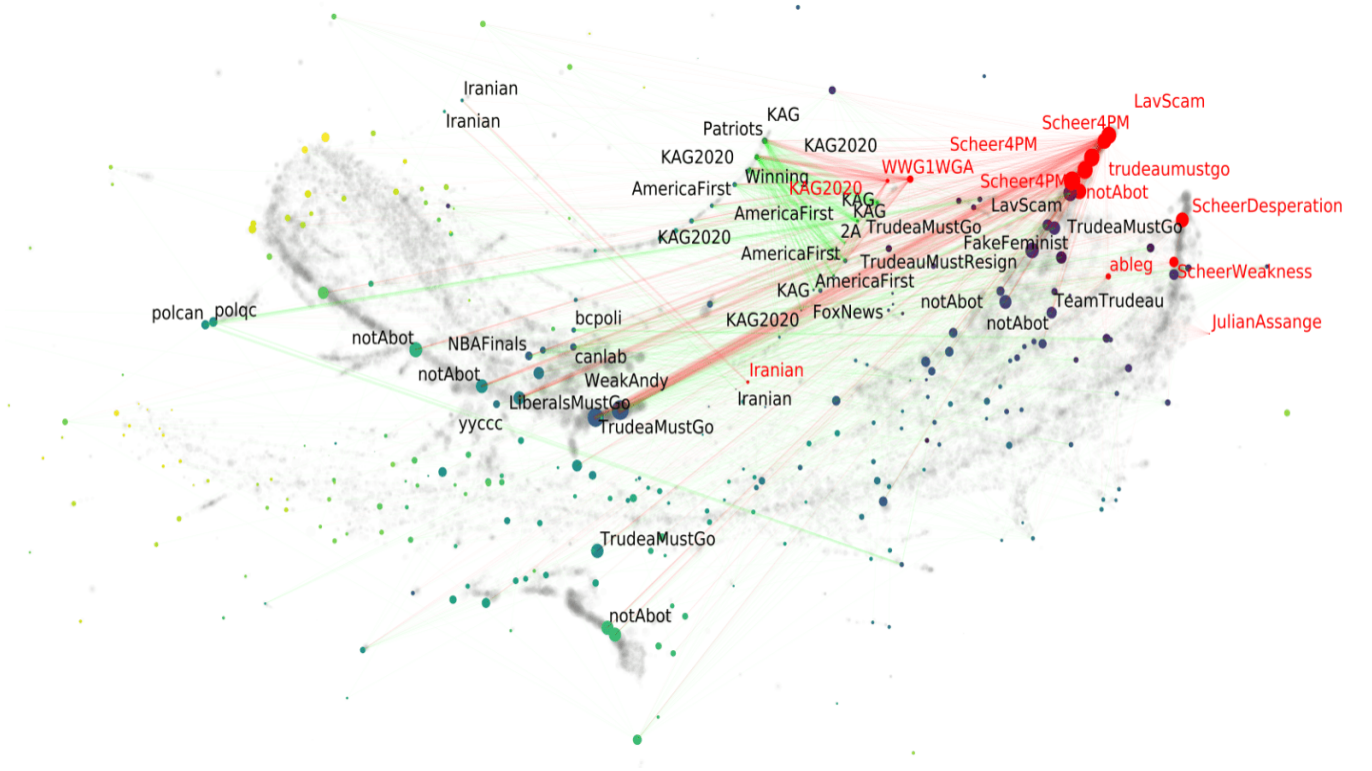


Figure 2: Map of twitter around 2019 Canadian Election created by SGP, which provides a birds eye view of how the detected polluting groups of users engage in the discourse. Each colored node represents a group of users who are behaving in a strikingly similar way. Size of group nodes corresponds to the group engagement in Canadian politics. Size of the background nodes represents individual level engagement of users whereas the density of the background corresponds to how many users are engaging in that space. Polluting groups are marked by red. All groups that are engaging significantly with rest of the map are tagged with their SGP-signature hashtag, and their outgoing edges are plotted to show the spread of their influence. Spread of the polluting groups is marked by red.

(2) message passing signals over G by summation aggregation. Note that we relax the procedure to binarize \mathbf{X} in step (1), because left singular values of \mathbf{X} could preserve more information than \mathbf{X}^b . As shown in experiments on synthetic data, this representation is very powerful for discovering tiny clusters.

More formally: given $G = (\mathcal{V}, \mathcal{E}, \mathbf{X})$, SGP-map embeds $v_i \in \mathcal{V}$ as $h_i \in \mathbf{H}$ by summation aggregation of one-hop neighbor's attributes

projected onto top- k left singular vectors:

$$h_i = \sum_{j \in \mathcal{N}(v_i)} \Pi_k x_j \quad (1)$$

In matrix form,

$$\mathbf{H} = \mathbf{A} \Pi_k \mathbf{X} \quad (2)$$

Given \mathbf{H} , SGP-map then applies a centroid or density based clustering algorithm to assign node embeddings $h_i \in \mathbf{H}$ to K partitions $\{U_1 \dots U_K\}$, thus rendering a coarsened map of the data.

SGP-flag detects polluting blocks in G by defining a metric ρ over graph G and subset of nodes $U \in \mathcal{V}$, and then flag subsets whose metric is above a threshold as polluting block. More formally given $G = (\mathcal{V}, \mathcal{E}, \mathbf{X})$, a disjoint covering partitions of $\mathcal{V} : \{U_1 \dots U_K\}$, and a threshold λ^* , SGP-flag marks each $U_i \in \{U_1 \dots U_K\}$ as suspicious if

$$\rho(G, U_i) \geq \lambda^* \quad (3)$$

If using edge probability:

$$\rho(G, U) = \frac{|\mathcal{E}(SU)|}{|\mathcal{V}(SU)| \times (|\mathcal{V}(SU)| - 1)}, \quad \lambda^* \in [0, 1] \quad (4)$$

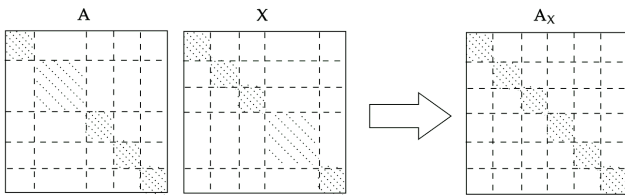


Figure 3: Resulting dense-block split \mathbf{A}_X given differently-sized dense-blocks on adjacency matrix \mathbf{A} and attribute matrix \mathbf{X} .

Symbols	Definitions
G	a directed attributed graph
\mathcal{V}	nodes
\mathcal{E}	edges
\mathbf{A}	adjacency matrix
\mathbf{X}	attribute matrix
\mathbf{H}	embedding matrix
$\llbracket f x \rrbracket$	element-wise function that binarizes $x \in \mathbf{X}$
\mathbf{X}^b	binarized \mathbf{X} after applying $\llbracket f x \rrbracket$
$\{U_1, \dots, U_K\}$	disjoint and covering partition of \mathcal{V}
$\{W_1, \dots, W_K\}$	partition of columns of \mathbf{X} or \mathbf{X}^b
P	edge probability matrix for partition $\{U_1, \dots, U_K\}$
p_U	edge probability for a subset of nodes $U \in \mathcal{V}$
λ	edge probability threshold
\mathcal{N}_v	one-hop neighborhood of node v
$\Pi_k \mathbf{X}$	projection of \mathbf{X} into its top k left singular value
$S'V'$	subgraph induced by $\mathcal{V}' \subseteq \mathcal{V}$

Table 1: Symbols and Definitions

Using this metric, the partitions returned by SGP-flag contain nodes that are well connected above λ , and also share significantly more homogeneous attribute relative to a random sample. Besides edge probability, other metrics such as conductance can be used, but we found edge probability to work best in both synthetic and real experiments.

SGP-map and SGP-flag together create a coarsened bird's eye view of the data with anomalies flagged.

SGP-signature creates a concise interpretable signature for each partition, both flagged and unflagged, by defining a metric over the binary attribute space and using it to rank the informativeness of each index $j \in 1 \dots d'$ of ordered attribute set W in terms of potentially explaining its overly homogeneous connection and attribute usage, and then creates signature for each partition by finding the most informative attribute.

More formally, given $G, \mathcal{V}, \mathcal{E}, \mathbf{X}$ and a disjoint covering partitions of $\mathcal{V} : \{U_1 \dots U_K\}$, and ordered attribute set W , SGP-signature defines a metric ϕ for each partition $U \in \{U_1 \dots U_K\}$ and index $j \in 1, \dots, d'$ of attribute set W as:

$$\phi W, U, j = \frac{i \in U \mathbf{X}_{ij}^b}{j' \in W i \in U \mathbf{X}_{ij'}^b} - \frac{i \in \mathcal{V} \mathbf{X}_{ij}^b}{j' \in W i \in \mathcal{V} \mathbf{X}_{ij'}^b} \quad (5)$$

this compares the local and global relative usage frequency of j . The group signature for U is simply derived as:

$$\operatorname{argmax}_j \phi W, U, j \quad (6)$$

Attribute j is the most informative attribute that characterize a partition U . The aforementioned three components of SGP are able to identify anomalous subgroups, as well as provide concise data summarization.

SGP-meso. defines a higher-order metric to characterize the strength of partition (group) interactions. More formally given $G, \mathcal{V}, \mathcal{E}, \mathbf{X}$ and a disjoint covering partitions of $\mathcal{V} : \{U_1 \dots U_K\}$, SGP-meso

defines a symmetrical pairwise metric over partitions:

$$\psi U_i, U_j = \frac{|\{v_l, v_r \in \mathcal{E} \mid v_l \in U_i, v_r \in U_j\}|}{|U_i| \times |U_j|} \quad (7)$$

ψ characterizes the strength of connection between a pairs of partitions.

These four components of SGP make it a powerful tool for joint anomaly detection and data summarization on attributed graphs. Next we demonstrate its effectiveness, scalability and interpretability with synthetic experiments and real-world data application.

3 EXPERIMENTS

In this section, we first verify the effectiveness of first two components of the proposed SGP method (SGP-map, SGP-flag) through a set of synthetic experiments with builtin ground-truth, which approximate the real-world problem and enable us to provide a quantitative evaluation. Next, we discuss the observations provided by applying all four components of SGP on real-world Twitter data and provide several evidences on the effectiveness of the SGP in unveiling the dynamics of polluting groups around the 2019 Canadian federal election.

3.1 Validation on Synthetic Data

Synthetic data model: We use stochastic block models [9] to synthesize data since they provide explicit control over dense block numbers, sizes and edge probabilities, as well as the background graph topology. To generate joint matrices, and without the loss of generality, we assume the dimension of the binary attribute matrix to be the same size as the total number of nodes in the graph. Then we create both the adjacency and binary attribute matrices using stochastic block-model. We consider two setting where the dense blocks agree (simple) or disagree (hard, when blocks splits into more). Figure 3 gives an example of the generated matrices.

Parameter settings: To evaluate SGP-map and SGP-flag on synthetic graphs which correspond to the real world Twitter graph, we consider 6 settings in which a small portion of the nodes are in dense blocks and the rest are not partitioned. The exact parameters are summarized in Table 2. For example in the first case, we create a graph with 1000 nodes, in which 150 nodes are assigned to dense clusters of size 30, each with edge probability of 0.4, while the rest of the graph is sparse with edge probability of 0.005. This matches what we observe in our Twitter data, where background edge probability is low and we are interested in finding small dense clusters of size $O(\log n)$. In the blocks-disagree case, for each block, we randomly sample from dense block size and edge probability options.

For all experiments, we set number of top left singular vectors for SGP-map's projection $k = 100$, and set the edge probability threshold of SGP-flag as $\lambda = 0.05$.

Illustration of results: As an example, Figure 4 shows SGP-map results on a synthetic graph of 1,250 nodes with 350 anomalies in dense blocks of sizes 50 and 100, and these blocks disagree on adjacency and attribute matrix, thus creating splits. The top row shows UMAP[17] 2-D visualization of SGP-map embeddings, colored from left to right by block partitions on adjacency, attribute, joint and inferred joint space. The bottom row shows the corresponding partitions on the attribute matrix on second column and adjacency

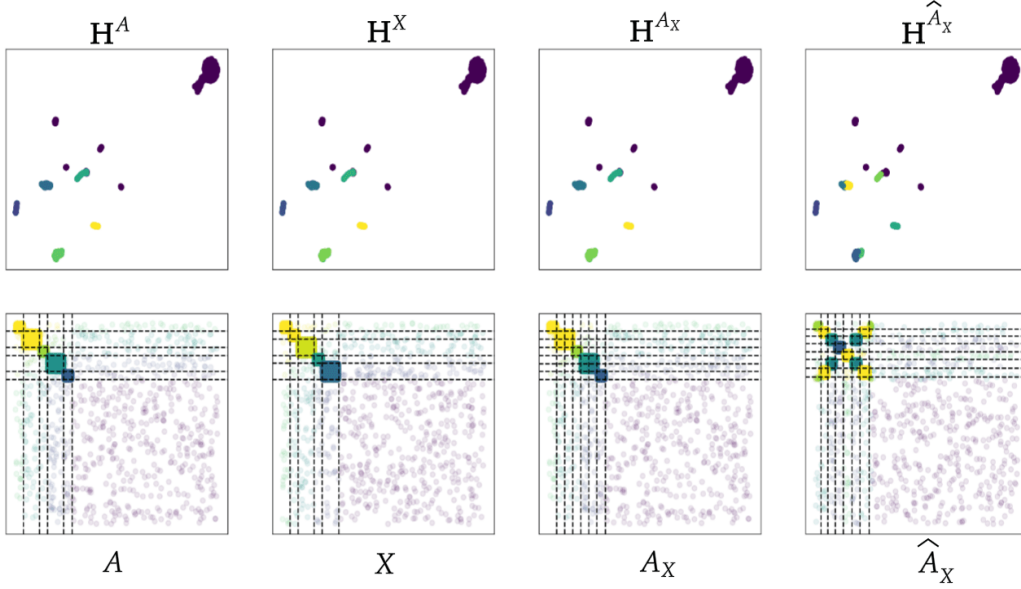


Figure 4: SGP-map recovers jointly dense blocks. Top: the embedding that separates the dense block. Bottom: the block structure in the corresponding matrices. A_X corresponds to the jointly dense blocks in A and X , plotted on A (ground-truth), and \hat{A}_X shows the blocks recovered by SGP-map (results).

Blocks-agree			
$ \mathcal{V} $	1,000	50,500	100,000
$p\mathcal{V}$	0.005	0.005	0.005
$i U_i $	150	235	300
$ U_i $	30	30	30
pU_i	0.4	0.4	0.4
Blocks-disagree			
$ \mathcal{V} $	1,000	50,500	100,000
$p\mathcal{V}$	0.005	0.005	0.005
$i U_i $	150	235	300
$ U_i $	20, 40	20, 40	20, 40
pU_i	0.1, 0.4, 0.7	0.1, 0.4, 0.7	0.1, 0.4, 0.7

Table 2: Parameters used for synthetic data generation

matrix on other columns. As shown on the bottom right corner of Figure 4, SGP-map is able to capture the injected dense blocks on the split level and thus forms block-diagonal structure on adjacency matrix ordered by the inferred joint partition.

Comparison with baselines: We compare against two contender methods from the classic and deep-learning based anomaly detection methods: Fraudar [10], a dense block detection heuristics-based algorithm that only uses adjacency matrix; and DOMINANT [7], which uses node reconstruction loss from graph convolution auto-encoder trained on both adjacency and attribute matrix. We also consider two variants of SVD -based embedding: (1) SVD_1 applies

truncated SVD on \mathbf{AX} directly without message passing step. SGP’s performance is comparable with SVD_1 but with much better scalability; (2) SVD_2 only uses sub-sampled nodes for truncated SVD. This provides a negligible speedup, however its performance drops significantly compared to SGP. Results are reported in Table 3.

We can see that SGP outperforms Fraudar even when not utilizing the attribute information (blocks-agree), in which case the attribute and adjacency matrices contain the same information. Results from DOMINANT are not reported in the table as it fails to converge on all the synthetic datasets. We observe that the convolutional graph auto-encoder training has high likelihood of divergence on sparse graphs with tiny dense blocks. We have also attempted using graph auto-encoder and variational graph auto-encoder [12] with different priors such as unit Gaussian and mixture of Gaussian on different graph neural net architectures including GraphSAGE [8] and graph attention network [30] for our embedding-based approach, but SGP beats their performance by a large margin, and hence the performance of these efforts are not reported. We conclude that for this specific task, SGP-map is superior to state-of-the-art deep learning based methods in terms of simplicity, scalability and performance. We find the embeddings created by SGP-map is the most powerful representation for discovering small blocks on sparse attributed graphs.

3.2 Performance on Real-World Data

Data collection: Since April 2019, we started collecting tweets related to 2019 Canadian federal election through the Twitter streaming API filtered by an evolving set of relevant hashtags based on

Metric	Blocks-agree				Blocks-disagree			
	ARI	NMI	F1	Time (s)	ARI	NMI	F1	Time (s)
1,000 nodes, 2,288 edges (15 % nodes in dense block)								
SGP	0.99 ± 0.00	0.98 ± 0.01	0.99 ± 0.00	0.20 ± 0.03	0.80 ± 0.15	0.75 ± 0.11	0.83 ± 0.13	0.21 ± 0.05
SVD ₁	0.99 ± 0.00	0.98 ± 0.01	0.99 ± 0.00	0.21 ± 0.04	0.80 ± 0.14	0.75 ± 0.10	0.83 ± 0.13	0.22 ± 0.06
SVD ₂	0.96 ± 0.05	0.95 ± 0.05	0.97 ± 0.04	0.17 ± 0.05	0.82 ± 0.12	0.77 ± 0.08	0.86 ± 0.11	0.23 ± 0.09
Fraudar	-	-	0.85 ± 0.27	0.06 ± 0.00	-	-	0.44 ± 0.01	0.06 ± 0.00
50,500 nodes, 1,277,467 edges, (0.47% dense block)								
SGP	0.93 ± 0.08	0.93 ± 0.08	0.93 ± 0.08	15.62 ± 1.44	0.52 ± 0.29	0.53 ± 0.28	0.52 ± 0.29	28.57 ± 9.66
SVD ₁	0.94 ± 0.07	0.92 ± 0.05	0.94 ± 0.07	95.89 ± 3.81	0.60 ± 0.16	0.63 ± 0.11	0.60 ± 0.16	121.95 ± 7.09
SVD ₂	0.27 ± 0.17	0.00 ± 0.00	0.27 ± 0.17	23.23 ± 3.98	0.29 ± 0.19	0.29 ± 0.17	0.29 ± 0.19	27.32 ± 3.10
Fraudar	-	-	0.01 ± 0.00	15.24 ± 0.20	-	-	0.01 ± 0.00	15.24 ± 0.20
100,000 nodes, 5,002,879 edges (0.25% nodes in dense block)								
SGP	0.45 ± 0.18	0.53 ± 0.12	0.46 ± 0.18	67.49 ± 4.32	0.61 ± 0.21	0.63 ± 0.17	0.61 ± 0.21	92.62 ± 23.95
SVD ₁	0.58 ± 0.13	0.62 ± 0.09	0.58 ± 0.13	1081.68 ± 160.23	0.64 ± 0.19	0.67 ± 0.14	0.65 ± 0.19	1143.04 ± 74.33
SVD ₂	0.03 ± 0.07	0.16 ± 0.00	0.03 ± 0.07	67.33 ± 5.16	0.14 ± 0.18	0.31 ± 0.02	0.14 ± 0.18	82.62 ± 9.31
Fraudar	-	-	0.00 ± 0.00	55.32 ± 0.50	-	-	0.00 ± 0.00	55.34 ± 0.30

Table 3: Performance on synthetic experiments. SGP-map: we evaluate our results using normalized mutual information (NMI) and adjusted random index (ARI) score of the inferred blocks versus the ground truth. **SGP-flag:** we also report the F1 score on whether the inferred partitions that are above our edge probability threshold correspond to the jointly dense blocks.

recent political events, the final set of hashtags is shown in Table 4. We refer to this set of hashtags as **Canadian hashtags**: W_C .

For each Twitter user that used any of the hashtags in table 4, we collected all usernames of his or her followers, as well as a sample of historical tweets between April and October 2019. This can be of different size for different users due to our data collection pipeline. For each user, we also tracked all hashtag usages in his or her sampled tweets, and created a feature vector where each entry is the frequency of using the corresponding hashtag.

#cdnpoli	#canpoli
#cpc	#SenCA
#cdnleft	#pttory
#ptbloc	#gpc
#crtc	#goc
#BlackFaceTrudeau	#TrudeauMustResign
#BlackFace	#BrownFace
#ScheerLies	#elxn43
#NotasAdvertised	#TrudeauTheHyprocite
#ptlib	#lpc
#ndp	#lavscam
#ptndp	#ptgreen
#cdnsen	#cpac
#CdesCom	#TrudeauBlackFace
#BrownFaceTrudeau	#TrudeauWorstPM
#Scheer	#Andysresume
#elxn43	#elxn19

Table 4: Hashtags used for crawling the data which are related to Canadian politics and the 2019 federal election.

We only keep users that tweeted at least once using a hashtag in W_C . Then we further filter this set to contain users who have at least 1 follower or follow at least 1 other user. The resulting directed

attributed graph G has $n = 69709$ nodes, $|\mathcal{E}| = 3480145$ edges and $d = 1329385$ unique hashtags.

Data preprocessing: Because entries of \mathbf{X} are highly skewed with some users using significantly more hashtags than others, and some hashtags significantly more popular than others, we apply doubly-normalized TF-IDF to give more importance to non-common hashtags, more specifically:

$$\mathbf{X}_{ij}^{tfidf} = \frac{n}{i' \in 1 \dots n} \frac{0.5}{\mathbf{X}_{i'j}^b} \frac{0.5 \mathbf{X}_{ij}}{\max_{j' \in 1 \dots d} \mathbf{X}_{ij'}} \quad (8)$$

where n is the total number of users, $\mathbf{X}^b = \llbracket \mathbf{X} > 0 \rrbracket$, and $i' \in 1 \dots n$ $\mathbf{X}_{i'j}^b$ shows in how many users used the hashtag j .

We consider the top 1,000 hashtags with highest mean TFIDF value to be **important hashtags**: W_I , which is used later for SGP-signature. We measure each user's **engagement with Canadian politics** by the ratio of at-least-once usage of Canadian hashtags:

$$f_{ev_i} = \frac{j \in W_C \mathbf{X}_{ij}^b}{|W_C|} \quad (9)$$

Given the resulted matrices of user followerships and hashtags, we performed preliminary exploratory analysis to discover anomalous patterns, including investigating how degree of nodes corresponds to the number of hashtags they use or their hashtag usage entropy. Given a considerable effort, this type of traditional feature-based anomaly detection did not yield any significant insight, and hence is omitted from the results. This however signifies the importance of applying the proposed SGP method, which we discuss next.

Applying SGP-map. Compared with synthetic data, some of the users in the twitter data don't have any followers and naive aggregation of signals would set them to 0, thus we relax SGP-map by message-passing on both \mathbf{A} and \mathbf{A}^T and then concatenate to form final node embedding:



Figure 5: SGP-map finds polluting groups of users exhibiting block-diagonal structure in both the adjacency (left) and attribute matrix (right) on the twitter data.

$$\tilde{\mathbf{H}} = (\mathbf{A}\Pi_k\mathbf{X}, \mathbf{A}^T\Pi_k\mathbf{X}) \quad (10)$$

Quality of the SGP-map. We first visualize subset of blocks identified by SGP-map in Figure 5, which shows a clear block structure for both \mathbf{A} (-diagonal) and \mathbf{X} on indices induced by these blocks, which indicates SGP-map’s ability to discover tightly connected user groups engaging with different sets of hashtags.

Next, we visualize the node embeddings resulted by SGP-map using UMAP projection to 2D in Figure 6. Size of the point for $v \in \mathcal{V}$ corresponds to $f_e v$, level of engagement in Canadian politics. Background nodes, those that do not get clustered into small clusters are plotted as grey with a lighter shade. Overlayed on each colored cluster of users U , is the most descriptive hashtag for that cluster, created by SGP-signature. We observe that SGP-map embeds groups with similar political creeds close to each other, thus forming an informative map of Twitter: top middle occupied by American conservative groups indicated by #KAG; the center by international groups signified by #Chinese, #Iranian, #Paris; top right by pro-Scheer and anti-Trudeau groups; the middle right by anti-Scheer groups; the middle left by climate activist groups, evidenced by #climate and #AmazonRainforest, etc.

Quality of the SGP-flag. Given the partitions $\{U_1, \dots, U_k\}$ created by SGP-map, SGP-flag sets edge probability threshold $\lambda = 0.01$ to flag subset of them as polluting. The block-diagonal adjacency matrix induced by the resulting 13 polluting blocks is visualized in Figure 1, where we observe siloed blocks such as #7, as well as interacting ones, #4 and #3, which are likely American conservative groups. Another observation is that the American conservative block #3 with four suspended users interacts with two smaller blocks with the hashtag signatures of #LavScam and #Scheer4PM, which are likely Canadian pro-Scheer and anti-Trudeau groups. This could be considered a potential foreign influence on the Canadian 2019 Election, which is concerning.

These 13 polluting blocks are marked as red in Figure 2, where we plot background nodes in the largest cluster similarly as in Figure 6; we also plot each other cluster U as a colored point, with size proportional to

$$\frac{\log|U| \sum_{v \in U} f_e v}{|U|} \quad (11)$$

which is an indicator of its engagement with Canadian politics on a group level. We can see that the 13 polluting blocks are highly engaged with Canadian politics, evidenced by their node size, and are close to each other in the embedding space.

We have observed that within these 13 polluting blocks, 9 out of 327 users are **suspended** in the past 6 months, which is over 4

times more compared to the other users. In total 429 out of 69,709 users in our data got suspended. Many users in these 13 polluting blocks, that are highly similar to those suspended accounts have not yet been identified and suspended by twitter. However, SGP-flag is able to spot these users who are behaving in the same manner as the suspended ones.

Quality of the SGP-signature. We apply SGP-signature to the set of important hashtags W_I and return $\arg\max_j \phi W_I, U, j$ defined in Equation 6, the signature that characterize the political creed of users in the group U . SGP-signature highlights the signature hashtag for each group in the the twitter maps of Figure 6 and 2. This characterizes the results in a concise manner, and explains the complex structure through which these groups are engaged in Canadian politics.

Contrasting fig. 7 and fig. 2, we observe that the signatures captured by SGP-flag on detected polluting blocks overlap with 8 out of 13 top suspended blocks’ signatures, including #Iranian, #KAG2020, #notAbot, #TrudeauMustGo and #Scheer4PM. This makes it a useful tool for spotting suspicious groups on social platforms. We also verify that two of these **hashtags discovered by SGP-signature are known to be linked to misinformation campaigns** [22, 18].

In particular, Figure 8 shows the relative group usage frequency for both Canadian hashtags and important hashtags for the SGP-flag-detected polluting block U_3 , which has the most suspended users. While block #3 is primarily an American conservative group by looking at the important hashtags, when zooming in on Canadian hashtags, a concerning observation emerges: this block of users has significantly more engagement with a specific Canadian hashtag: #TrudeauMustGo, which has been very recently found to be related to trending misinformation campaign against Candian 2019 Election [22]. Furthermore, another signature picked up by SGP-signature (#NotAbot) in the polluting blocks identified by SGP-map and SGP-flag has also been reported to engage in information campaign [22].

These two hashtags have so far been the primarily used hashtag against 2019 Canadian election, and both have been detected before mainstream media coverage. This makes SGP-signature a powerful tool to assist in detecting trending misinformation campaigns before they make significant mark.

Quality of the SGP-meso. SGP-meso quantifies the strength of connection among all clusters, and thus enables the study of their spread and potential success. In figure 2, link between two clusters U_i, U_j is plotted with line width proportional to their interaction $\psi U_i, U_j$ defined in Equation 7; those that are connected to detected 13 polluting blocks are colored red, and other links are plotted as green. For any cluster U_i with $\max_j \psi U_i, U_j, i \neq j$ greater than a threshold, we overlay its SGP-signature signature on top.

One concerning observation from SGP-meso result is the obvious existence of a large international right-wing group spanning across America and Canada that actively engages with and potentially influences the Canadian 2019 Election. Their signature hashtags include #Scheer4PM, #KAG2020, #TrudeauMusGo, #LiberalsMustGo, etc. Another such concerning observation is the existence of aforementioned signature #notAbot, where almost all groups with this signature are linked with the detected 13 polluting blocks. Such homogeneity could be a sign of a misinformation campaign.

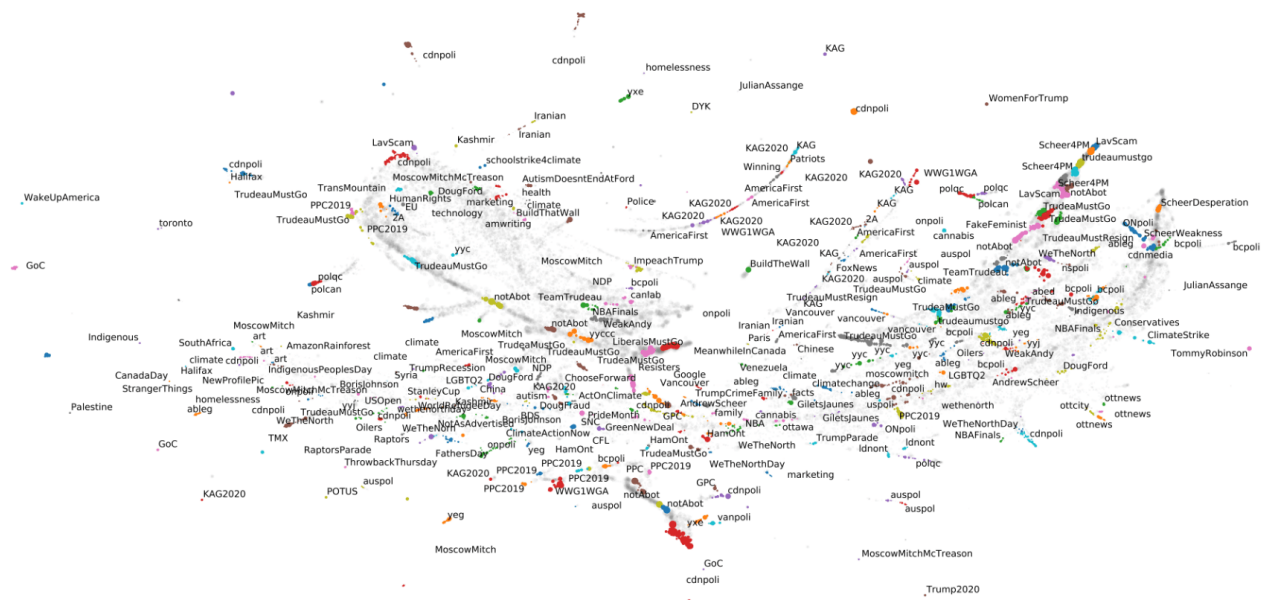


Figure 6: SGP-map puts users of the same political creed close together. Here nodes are the individual users, size of the nodes corresponds to the level of engagements of that particular node in the Canadian politics. Nodes are colored the same if they belong to the same micro-cluster.

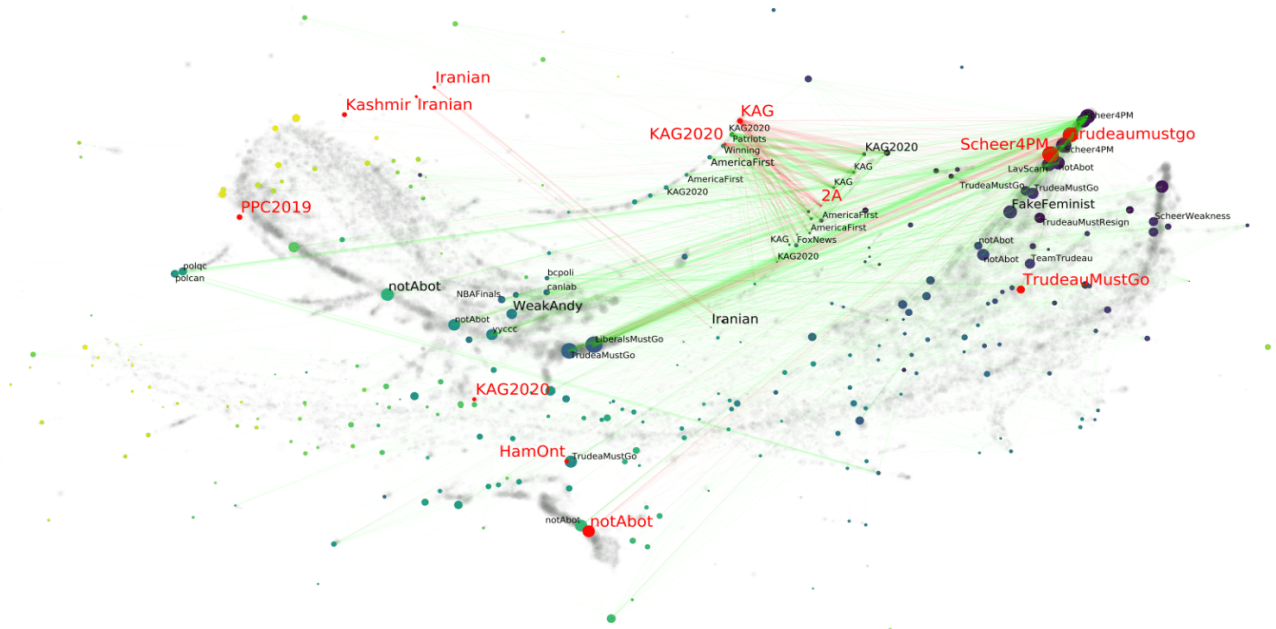


Figure 7: SGP-flag results corroborates with the users suspended by Twitter. Text size corresponds to the ratio of suspended users within all our detected group, whereas the size of the node corresponds to their level of engagement in the Canadian politics similar to fig. 2. Groups colored as red are the top 13 groups with the highest ratio of suspended users.

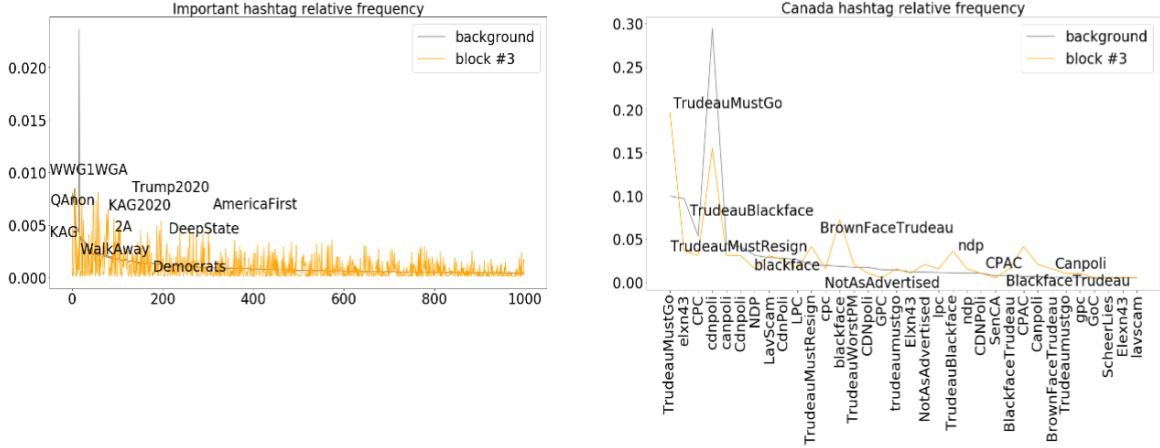


Figure 8: SGP-signature finds informative hashtag in both important hashtag set (left) and Canadian hashtag set (right) for polluting block #3. Plotted for both sides are top 10 hashtags that are used by block #3 more often on a group basis than the background.

Less concerning but still interesting observation emerge when inspecting Figure 2 and 7 side by side, where SGP-flag identifies one out of three blocks signatored by #Iranian, and top suspension ratio reveals the other two blocks signatored by #Iranian. Yet there is no significant connections going outside of these three groups to other parts of the graph. Inspection of the users' tweets in these clusters reveals that the accounts in these blocks are primarily concerned with immigration issues and are mostly created in February 2019, right before the passing of Bill 21, a Bill in Quebec that sets out framework for values test for skilled workers, which impacts immigration. The observed strong connection within a set of groups but weak or no connection to other parts of a graph, could be a sign of a failed amplifying strategy.

Scalability of SGP:. Here we analyze time complexity of SGP. The bulk of computation done by SGP are:

- Computing truncated singular value decomposition of a large sparse attribute matrix $\mathbf{X} \in \mathbb{R}^{n \times d}$. $|\cdot|$ denotes number of nonzero entries in a sparse matrix. For large sparse matrices, augmented Lanczos bidiagonalization algorithm [4] is the default option for computing truncated singular value decomposition, whose time complexity is $OT|\mathbf{X}|k^3c$, where $|\mathbf{X}|$ is nonzero entries in \mathbf{X} , T is number of iterations, k is number of top left singular vectors to project \mathbf{X} and c is constant. When $k \ll n$, the time complexity is approximately $O|\mathbf{X}|$.
- Computing sparse matrix product between \mathbf{A} and $\Pi_k \mathbf{X}$, whose time complexity is $O|A|k$ for standard implementation, k as mentioned above.

Thus the resulting complexity of SGP is $Omax|A|, |X|$. Assuming $|A|$ and $|X|$ are in the same range, SGP scales linearly with the number of edges in G . It is able to analyze realistic graph of size 100,000 in less than **2 minutes on a normal laptop**.

4 CONCLUSIONS

In this paper we presented SGP, which discovers, characterizes and explains polluting groups in social media platforms. SGP is

Holistic: SGP jointly models user's connection and content, i.e. it exploits both attribute and structural information, hence is able to uncover patterns at the high level and provide bird's eye view of the activities in a social platform.

Effective: SGP performs better than both classic and deep-learning based baselines by a large margin. It is also able to identify polluting groups that are over 4 times more likely to get suspended.

Interpretable: As shown in Figure 2, the four components of SGP gives a concise summarization of complex interaction dynamics of normal and anomalous groups on Twitter, and is able to capture groups engaging in misinformation campaign, as well as how they interact with each other before mainstream media.

Scalable: SGP scales linearly with number of edges with reasonable assumptions.

Reproducible: We will open-source our code after acceptance.

5 BACKGROUND AND RELATED WORK

There are many works that this paper builds upon. Here we briefly discuss the most relevant papers to understanding social media ecosystems, detecting anomalous users (e.g. bots, trolls) and how they interact with democracy and politics. We also highlight the most relevant papers to the methodology used to embed graph information (e.g. graph representation learning), and detect coordinated activity in these platforms (e.g. community detection, anomaly detection).

5.1 Online Misinformation

According to recent work on network theory [2, 20, 33], the vulnerability of social networks to information operations relates to the clustering of politicised online information spaces. This phenomenon, defined as "echo-chambers", describes the gathering of like-minded individuals into online communities. As illustrated by Marwick *et al* [16], the defiance toward traditional media from part of the population leads to the emergence of alternative (possibly biased or fake) news sources. Analysing the fake news spreading processes on Twitter, Bovet *et al* [3] showed that trolls tend to map into small, politically biased networks of users, fed with multiple

Method \ Property	Fraudar [10]	Dominant [7]	DeepFD [31]	EigenSpoke [24]	GNN-based methods	pcv [21]	SGP
Attribute		✓	✓		✓		✓
Effectiveness			✓	✓		✓	✓
Scalability	✓		✓	✓		✓	✓
Interpretability			✓	✓			✓

Table 5: SGP matches all specs, while competitors miss one or more of the features.

information sources, thus making normal users sensitive to hostile influence. Indeed, Stewart *et al* [28] identified trolls as polarising elements of echo-chambers, distorting the information space. Therefore, we hypothesise that trolls ground their activity mainly within small networks of densely connected users, while being active on politicised discussions to further polarise edge individuals.

5.2 Community Detection

Community detection in networks is a task that involves finding community structures within graphs. In particular, the problem involves a set of node classification tasks that attempt to ascertain an underlying clustered, segmented and relatively dense structure within a graph. Traditional approaches like modularity maximization, which measures the number of edges in identified communities in relation to the expected number of edges in an unorganized graph, suffer from small-resolution communities and do not scale well to contemporary social networks [14]. More recent research has identified the need for combining both the underlying structure of the nodes within the network as well as their inherent attributes [15]. Liu *et al* [15] adopt the paradigm that a network graph results from interactions among nodes, and introduce the idea of content and influence propagation via random walks, analyzing the stable structure of this dynamical system to identify communities. Jia *et al* [11] enhance node attributes by running k-nearest neighbors on the graph a priori and append this information to node representations, demonstrating that this alleviates graph sparsity issues and improves performance of community identification algorithms. Most recently, graph neural networks (GNNs) extends the convolutional neural network framework to graph structures by leveraging affine transformations of graph operators and node-wise or edge-wise activation functions. Chen *et al* [6] introduce a new family of GNNs which rely on a non-backtracking graph operator defined on the line graph of edge adjacencies, facilitating scalable inference of communities on large, sparse graphs. A separate line of work aims to detect tiny communities. Neumann proposed an elegant and simple algorithm for provably finding community of size On^ϵ in a bipartite graph generated by bipartite stochastic blockmodel, by first clustering left-side nodes based on similarity of their neighbors, and then recover right-side partition based on degree thresholding [21].

5.3 Anomaly Detection

Anomaly detection is a well researched problem, but many techniques fail to be applicable on the extremely sparse graphs with a

large set of nodes which characterize most modern social networks. ODDBALL is a classical approach that defines several metrics surrounding the density, weight, rank and eigenvalues associated with anomalous subgraphs, and computes these measures to identify anomalous blocks [1]. Another approach is presented in [24] which detects persistent patterns, called EigenSpokes, which are found in large sparse social graphs. By plotting the singular vectors of these graph against each other (called EE-plots), clear, separate lines or spokes that often align with axes (EigenSpokes) are detected. EE-plots are indicative of fundamental clustering structures within these graphs. Alternatively, matrix factorization approaches have been extremely prolific in anomaly detection literature. For example, Tong and Lin adapt non-negative matrix factorization (NMF) by enforcing constraints to identify anomalies in the residual graph after typical factorization, thereby capturing anomalies in the original whole graph [29]. In line with recent advances involving deep learning, a major contribution in anomaly detection follows from DeepFD, an architecture developed by Wang *et al* based on graph embeddings of both attributed and topological graphs [32]. Their work preserves graph structure and user behavior in order to improve adversarial robustness to fraudsters within networks of interest. With the popularization of graph neural networks, graph convolutional autoencoder that encodes and decodes both adjacency and attribute matrix is used to rank nodes in terms of anomaly, indicated by node reconstruction error [7].

5.4 Dense Block Detection

The kind of lockstep behavior exhibited by agents who engage in information operations induces dense subgraphs within the larger graph [26], [25], [27]. While such blocks are locally dense, they are often extremely sparse the relative to the entire graph, and thus detection can be a difficult task. M-Zoom is a classical approach to this problem, which iteratively finds and removes dense blocks to prevent duplicate block querying [26]. Shin *et al* take an offline approach to the task in D-Cube, facilitating distributed, fast detection of dense blocks with provable guarantees on the accuracy of identifying blocks [27].

5.5 Graph Representation Learning

Graph representation learning aims to embed node, subgraph or the whole graph onto Euclidean space. This type of learning is inherently difficult as graphs are combinatorial structures with discretized nodes and edges. Thus, conventional learning modalities like neural networks often fail for these learning tasks as they rely on continuous representations of data. In particular, unsupervised graph representation learning is interesting as most graphs are not fully specified; connections between nodes within our data are often hidden or unknown, particularly in large scale graph structures such as social media networks. To this end, Kipf and Welling [12] develop the variational graph autoencoder that uses a graph convolutional network as an encoder which parameterizes a Gaussian latent distribution. A decoder network then reconstructs the full graph, and the authors demonstrate that such reconstruction from the latent embeddings predicts unseen or masked links in the original network with good accuracy. Moreover, their framework can be trained end to end through classical variational inference. More recently, Hamilton

et al. demonstrate greatly improved performance through their more general GraphSAGE approach [8]. GraphSAGE is able to perform inductive learning and generate node embeddings for previously unseen graphs. Critically, even in settings where node attributes are not made explicitly available, the GraphSAGE is extendable by computing additional node features such as degree from the network topology and substituting these as the node attributes.

REFERENCES

- [1] L. Akoglu, M. McGlohon, and C. Faloutsos. Oddball: Spotting anomalies in weighted graphs. In *Pacific-Asia Conference on Knowledge Discovery and Data Mining*, pages 410–421. Springer, 2010.
- [2] A. Badawy, E. Ferrara, and K. Lerman. Analyzing the digital traces of political manipulation: The 2016 russian interference twitter campaign. In *2018 IEEE/ACM International Conference on Advances in Social Networks Analysis and Mining (ASONAM)*, pages 258–265. IEEE, 2018.
- [3] A. Bovet and H. A. Makse. Influence of fake news in twitter during the 2016 us presidential election. *Nature communications*, 10(1):7, 2019.
- [4] A. Butler, P. Hoffman, P. Smibert, E. Papalexi, and R. Satija. Integrating single-cell transcriptomic data across different conditions, technologies, and species. *Nature biotechnology*, 36(5):411, 2018.
- [5] N. Chavoshi, H. Hamooni, and A. Mueen. Identifying correlated bots in twitter. In *International Conference on Social Informatics*, pages 14–21. Springer, 2016.
- [6] Z. Chen, X. Li, and J. Bruna. Supervised community detection with line graph neural networks. *arXiv preprint arXiv:1705.08415*, 2017.
- [7] K. Ding, J. Li, R. Bhanushali, and H. Liu. Deep anomaly detection on attributed networks. 2019.
- [8] W. Hamilton, Z. Ying, and J. Leskovec. Inductive representation learning on large graphs. In *Advances in Neural Information Processing Systems*, pages 1024–1034, 2017.
- [9] P. W. Holland, K. B. Laskey, and S. Leinhardt. Stochastic blockmodels: First steps. *Social networks*, 5(2):109–137, 1983.
- [10] B. Hooi, H. A. Song, A. Beutel, N. Shah, K. Shin, and C. Faloutsos. Fraudar: Bounding graph fraud in the face of camouflage. In *Proceedings of the 22nd ACM SIGKDD International Conference on Knowledge Discovery and Data Mining*, pages 895–904. ACM, 2016.
- [11] C. Jia, Y. Li, M. B. Carson, X. Wang, and J. Yu. Node attribute-enhanced community detection in complex networks. *Scientific reports*, 7(1):2626, 2017.
- [12] T. N. Kipf and M. Welling. Variational graph auto-encoders. *arXiv preprint arXiv:1611.07308*, 2016.
- [13] S. Kumar, J. Cheng, J. Leskovec, and V. Subrahmanian. An army of me: Sockpuppets in online discussion communities. In *Proceedings of the 26th International Conference on World Wide Web*, pages 857–866. International World Wide Web Conferences Steering Committee, 2017.
- [14] A. Lancichinetti and S. Fortunato. Limits of modularity maximization in community detection. *Physical review E*, 84(6):066122, 2011.
- [15] L. Liu, L. Xu, Z. Wangy, and E. Chen. Community detection based on structure and content: A content propagation perspective. In *2015 IEEE International Conference on Data Mining*, pages 271–280. IEEE, 2015.
- [16] A. Marwick and R. Lewis. Media manipulation and disinformation online. *New York: Data & Society Research Institute*, 2017.
- [17] L. McInnes, J. Healy, and J. Melville. Umap: Uniform manifold approximation and projection for dimension reduction. *arXiv preprint arXiv:1802.03426*, 2018.
- [18] E. McIntosh. A fake justin trudeau sex scandal went viral. canada’s election-integrity law can’t stop it. *News, Politics, Canada’s National Observer*. URL <https://www.nationalobserver.com/2019/10/10/news/fake-justin-trudeau-sex-scandal-went-viral-canadas-election-integrity-law-ca>
- [19] F. McSherry. Spectral partitioning of random graphs. In *Proceedings 42nd IEEE Symposium on Foundations of Computer Science*, pages 529–537. IEEE, 2001.
- [20] A. Mitchell, J. Gottfried, J. Kiley, and K. E. Matsa. Political polarization and media habits. *Pew Research Center*, Oct 2014. URL <https://www.journalism.org/2014/10/21/political-polarization-media-habits/>.
- [21] S. Neumann. Bipartite stochastic block models with tiny clusters. In S. Bengio, H. Wallach, H. Larochelle, K. Grauman, N. Cesa-Bianchi, and R. Garnett, editors, *Advances in Neural Information Processing Systems 31*, pages 3867–3877. Curran Associates, Inc., 2018. URL <http://papers.nips.cc/paper/7643-bipartite-stochastic-block-models-with-tiny-clusters.pdf>.
- [22] C. Orr. A new wave of disinformation emerges with anti-trudeau hashtag. *Election Integrity Reporting Project, Canada’s National Observer*. URL <https://www.nationalobserver.com/2019/07/25/analysis/new-wave-disinformation-emerges-trudeaumustgo>.
- [23] T. P. Policy. Update on twitter’s review of the 2016 us election. *Retrieved April*, 15:2018, 2018.
- [24] B. A. Prakash, A. Sridharan, M. Seshadri, S. Machiraju, and C. Faloutsos. Eigenspokes: Surprising patterns and scalable community chipping in large graphs. In *PAKDD (2)*, volume 6119 of *Lecture Notes in Computer Science*, pages 435–448. Springer, 2010.
- [25] K. Shin, T. Eliassi-Rad, and C. Faloutsos. Corescope: graph mining using k-core analysis patterns, anomalies and algorithms. In *2016 IEEE 16th International Conference on Data Mining (ICDM)*, pages 469–478. IEEE, 2016.
- [26] K. Shin, B. Hooi, and C. Faloutsos. M-zoom: Fast dense-block detection in tensors with quality guarantees. In *Joint European Conference on Machine Learning and Knowledge Discovery in Databases*, pages 264–280. Springer, 2016.
- [27] K. Shin, B. Hooi, J. Kim, and C. Faloutsos. D-cube: Dense-block detection in terabyte-scale tensors. In *Proceedings of the Tenth ACM International Conference on Web Search and Data Mining*, pages 681–689. ACM, 2017.
- [28] L. G. Stewart, A. Arif, and K. Starbird. Examining trolls and polarization with a retweet network. 2018.

- [29] H. Tong and C.-Y. Lin. Non-negative residual matrix factorization with application to graph anomaly detection. In *Proceedings of the 2011 SIAM International Conference on Data Mining*, pages 143–153. SIAM, 2011.
- [30] P. Veličković, G. Cucurull, A. Casanova, A. Romero, P. Lio, and Y. Bengio. Graph attention networks. *arXiv preprint arXiv:1710.10903*, 2017.
- [31] H. Wang, C. Zhou, J. Wu, W. Dang, X. Zhu, and J. Wang. Deep structure learning for fraud detection. In *2018 IEEE International Conference on Data Mining (ICDM)*, pages 567–576, Nov 2018. doi: 10.1109/ICDM.2018.00072.
- [32] H. Wang, C. Zhou, J. Wu, W. Dang, X. Zhu, and J. Wang. Deep structure learning for fraud detection. In *2018 IEEE International Conference on Data Mining (ICDM)*, pages 567–576. IEEE, 2018.
- [33] T. Wilson, K. Zhou, and K. Starbird. Assembling strategic narratives: Information operations as collaborative work within an online community. *Proceedings of the ACM on Human-Computer Interaction*, 2(CSCW):183, 2018.